Stem Cell Reports, Volume *10*

Supplemental Information

Histone 2B-GFP Label-Retaining Prostate Luminal Cells Possess Progenitor Cell Properties and Are Intrinsically Resistant to Castration

Dingxiao Zhang, Collene Jeter, Shuai Gong, Amanda Tracz, Yue Lu, Jianjun Shen, and Dean G. Tang

Supplementary Data

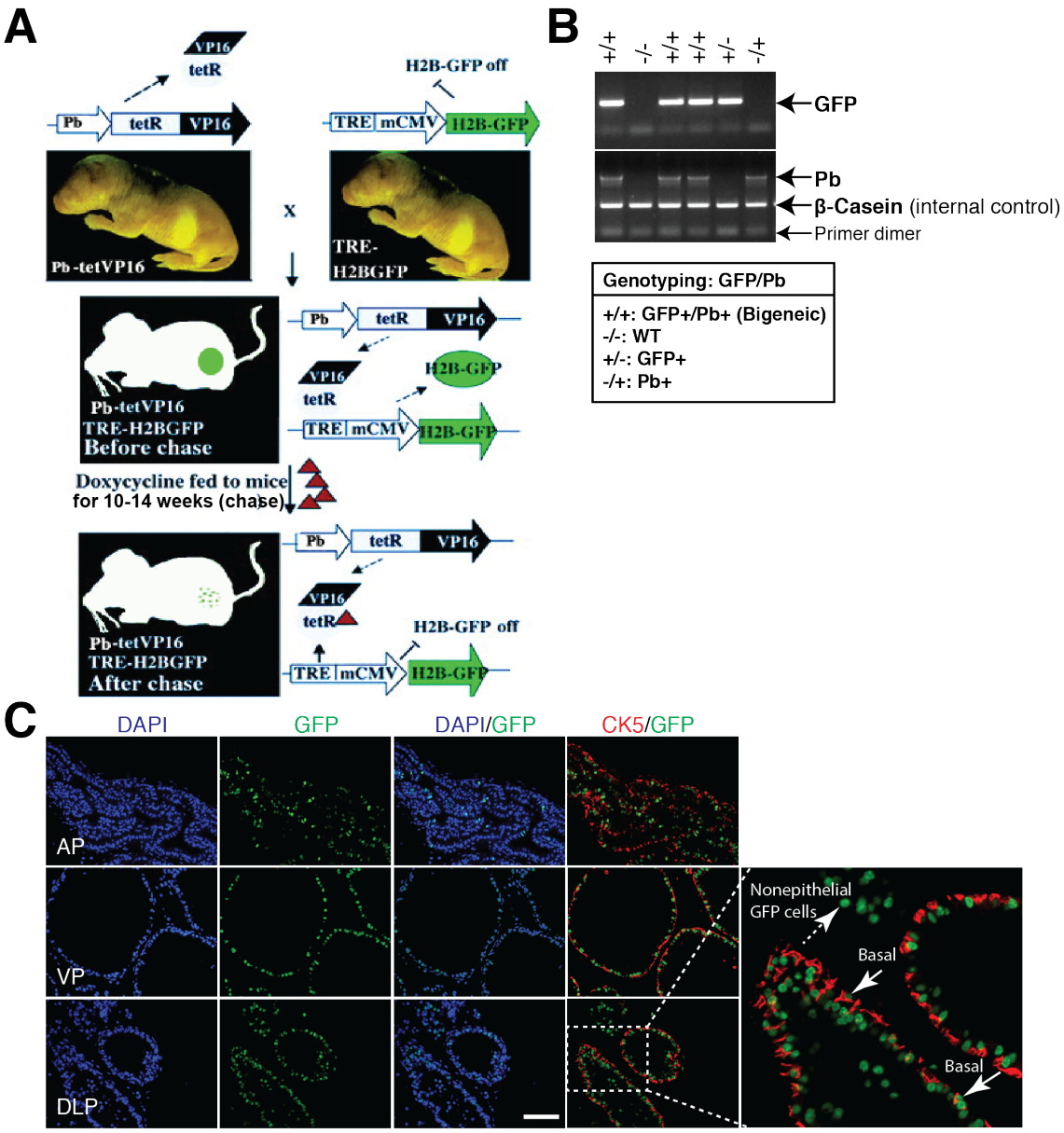

Figure S1. Establishment of a bigenic mouse model to label slow-cycling cells (LRCs) in the prostatic epithelium, Related to Figure 1

(A) Strategy to generate Pb-tetVP16-GFP bigenic mouse model (see Supplemental Experimental Procedures for detail).

(B) PCR genotyping of single and bigenic Pb-tetVP16-GFP mice.

(C) IF staining of CK5 and GFP in different prostate lobes dissected from unchased adult bigenic mouse identifying GFP^{+} basal cells and nonepithelial stromal cells. Boxed regions are enlarged. Scale bar, 100 μm.

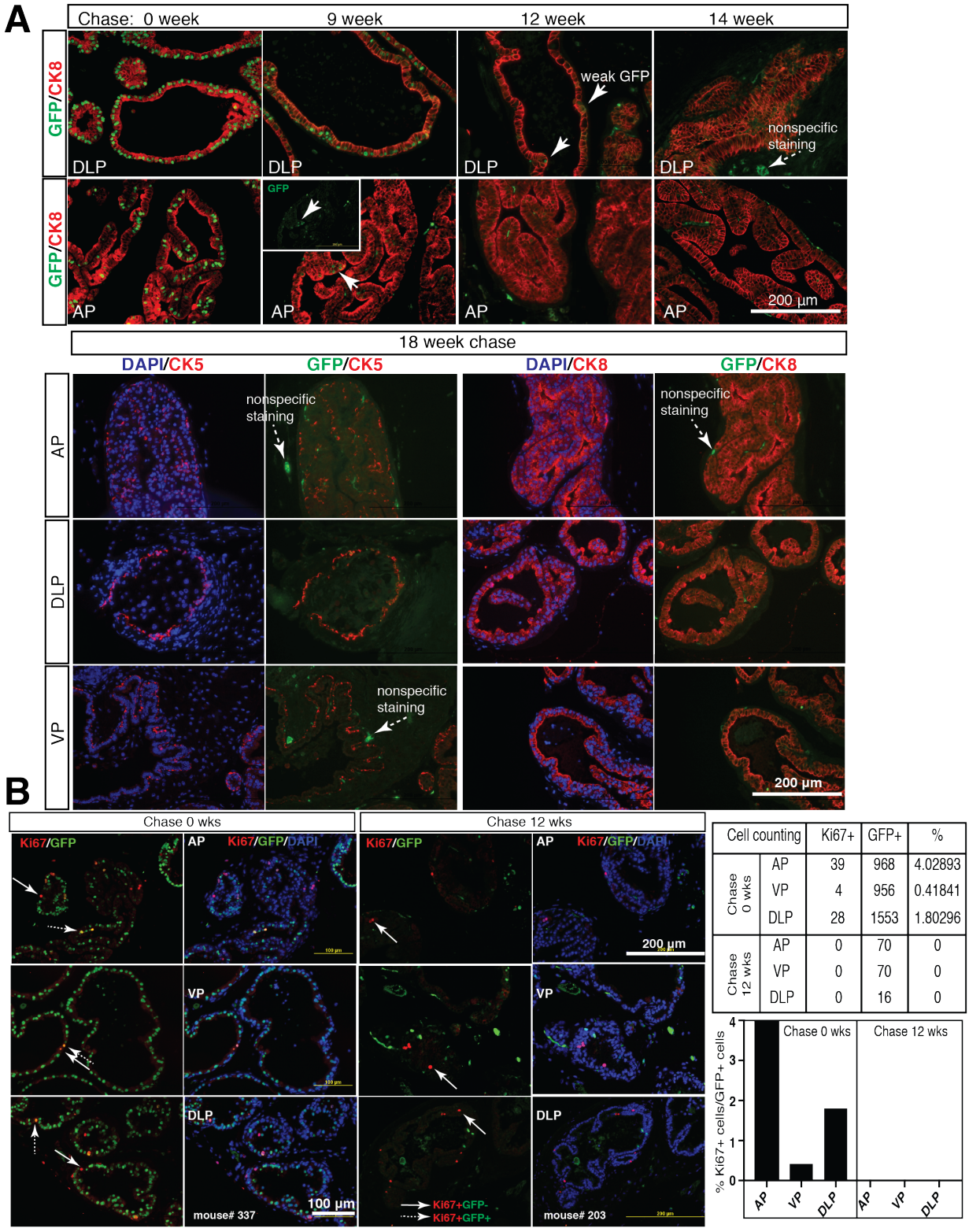

Cell counting		Ki67+	GFP+	%
Chase 0 wks	AP	39	968	4.02893
	VP	4	956	0.41841
	DLP	28	1553	1.80296
Chase 12 wks	AP	0	70	0
	VP	0	70	0
	DLP	0	16	0

Figure S2. Phenotypic characterization and quiescence of prostate LRCs, Related to Figure 2

(A) Double IF staining of CK5 or CK8 and GFP in different prostate lobes harvested from bigenic mice chased for 0 - 18 weeks. Arrows and dashed arrows indicate positive and non-specific GFP staining, respectively.

(B) Double IF of Ki67 and GFP in different prostate lobes of bigenic mice chased for 0 week and 12 weeks. Representative low-magnification images (left) and quantification data (right) are shown. Arrows and dashed arrows indicate $Ki67^{+}GFP^{-}$ single positive and $Ki67^{+}GFP^{+}$ double positive cells, respectively.

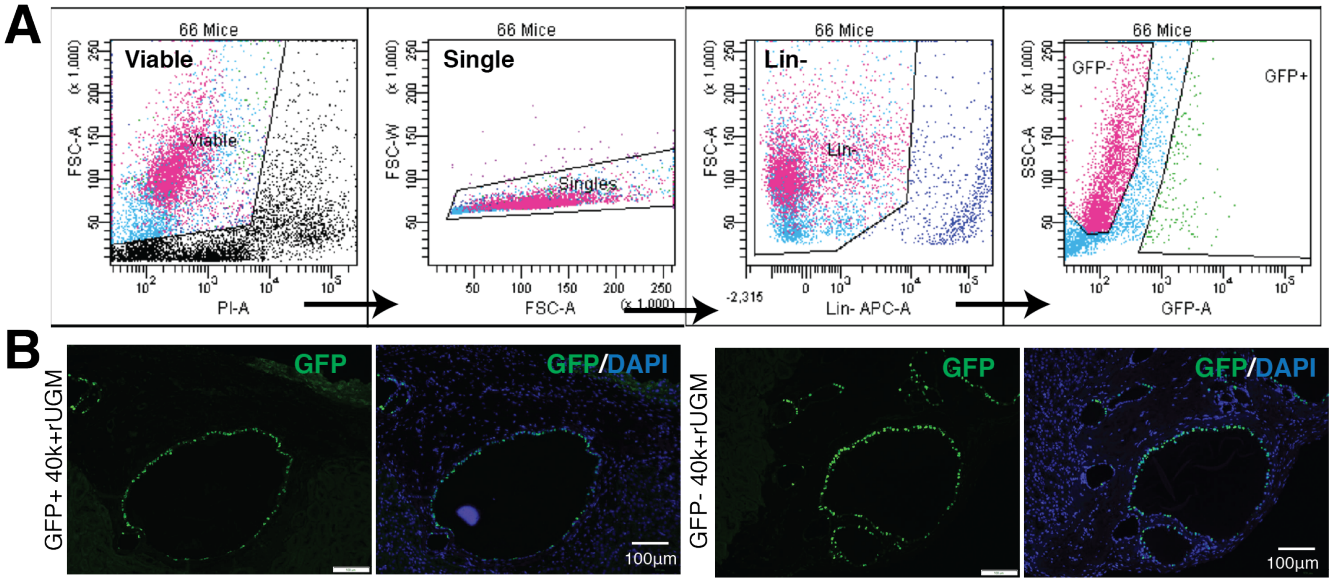

Figure S3. LRCs can regenerate prostate glands *in vivo*, Related to Figure 3

(A) Sorting strategy to isolate lineage-negative GFP^+ and GFP^- cells from disassociated bulk prostatic cells.

(B) IF of GFP in recombinants showing that both LRCs and non-LRCs can regenerate prostate tissues *in vivo*. Note that as we used a Tet-off system, the GFP^- cells isolated from 12-week chased animals (non-LRCs) would regain the GFP expression during the tissue regeneration assays.

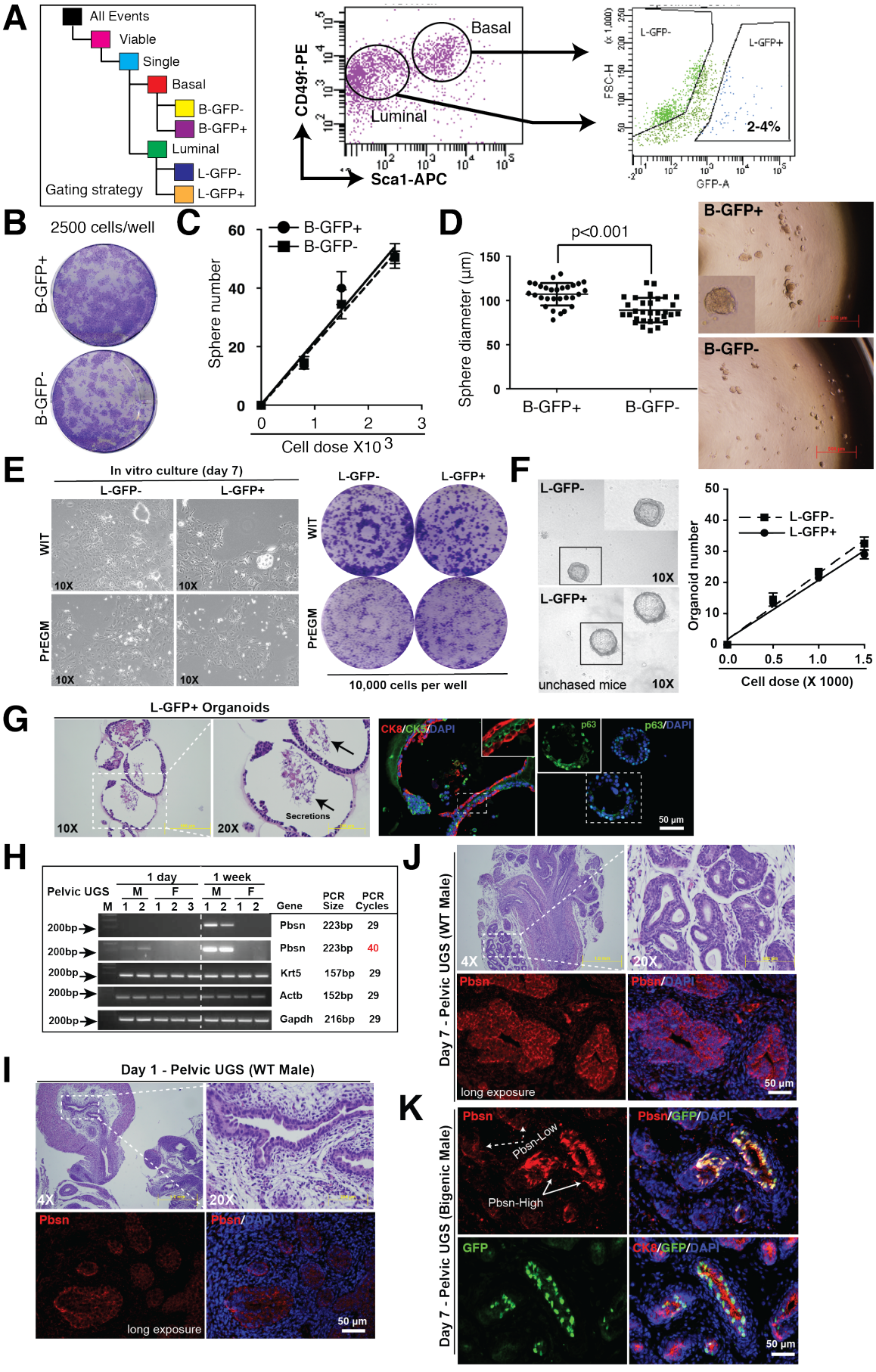
A
All Events
Viable
Single
Basal
B-GFP-
B-GFP+
Luminal
L-GFP-
L-GFP+
Gating strategy
CD49f-PE
Sca1-APC
Basal
Luminal
FSC-H
GFP-A
L-GFP-
L-GFP+
2-4%
B
2500 cells/well
B-GFP+
B-GFP-
C
B-GFP+
B-GFP-
Sphere number
Cell dose X10 3
D
p<0.001
Sphere diameter (µm)
B-GFP+
B-GFP-
B-GFP+
B-GFP-
E
In vitro culture (day 7)
L-GFP-
L-GFP+
WIT
PrEGM
10X
L-GFP-
L-GFP+
WIT
PrEGM
10,000 cells per well
F
L-GFP-
L-GFP+
10X
unchased mice
Organoid number
Cell dose (X 1000)
G
L-GFP+ Organoids
10X
20X
Secretions
CK8/CK5/DAPI
p63
p63/DAPI
50 µm
H
Pelvic UGS
1 day
1 week
M
F
Gene
PCR Size
PCR Cycles
200bp
Pbsn 223bp 29
Pbsn 223bp 40
Krt5 157bp 29
Actb 152bp 29
Gapdh 216bp 29
I
Day 1 - Pelvic UGS (WT Male)
4X
20X
Pbsn
Pbsn/DAPI
long exposure
50 µm
J
Day 7 - Pelvic UGS (WT Male)
4X
20X
Pbsn
Pbsn/DAPI
long exposure
50 µm
K
Day 7 - Pelvic UGS (Bigenic Male)
Pbsn
Pbsn-Low
Pbsn-High
Pbsn/GFP/DAPI
GFP
CK8/GFP/DAPI
50 µm

Figure S4. Luminal LRCs, but not basal LRCs, exhibit preferential stem/progenitor activities compared to non-LRCs, Related to Figure 4

(A) FACS strategy to isolate GFP^+ and GFP^- epithelial cells form both basal and luminal cell populations.

(B-D) Basal GFP^+ LRCs demonstrate similar sphere-forming efficiency to basal GFP^- non-LRCs. Freshly purified Lin^- prostate basal GFP^+/GFP^- cells ($B\text{-}GFP^+/B\text{-}GFP^-$) from 12 week-chased animals were used in colony formation (B) and limiting dilution sphere (C) assays. Note that $B\text{-}GFP^+$ cells did generate larger spheres than $B\text{-}GFP^-$ cells (D). Results shown were representative data of at least 2 independent experiments. The P value was calculated using Student's t-test. For (C) and (D), data represent mean ± SD of values obtained from one experiment.

(E, F) Freshly purified luminal GFP^+ and GFP^- cells from unchased adult animals exhibit similar stem/progenitor cell activities. Shown are 2D colony formation (E) and 3D organoid (F) assays. Pictures in E (left panel) confirmed the epithelial identify of the cells cultured in the indicated medium. Results shown were representative data of at least 2 independent experiments.

(G) Luminal LRCs isolated from 12 week-chased bigenic mice generated organoids containing both basal and luminal cells. Shown are H&E staining and IF analysis of p63, CK5 and CK8 in organoids.

(H) Semi-quantitative RT-PCR of *Pbsn* mRNA in pelvic urogenital sinus (UGS) isolated from newborn and 1-week old mice.

(I, J) H&E staining and IF analysis of Pbsn in pelvic UGS of newborn (I) and 1-week old WT mice (J) showing the minimal and considerable expression of Pbsn at protein level in newborn and 1-week old mice, respectively.

(K) Double IF analysis of GFP and Pbsn or CK8 in pelvic UGS of 1-week old bigenic mice.

Boxed regions are enlarged.

A

	RNA-seq	
	L_GFP-	L_GFP+
total number of fragments	73665989	80259391
fragments with both ends mapped	64184312	69737172
	87%	87%
fragments with one end mapped	4332527	4982840
	6%	6%
tags that are not mapped	14630827	16061598
total mapped rate	93%	93%

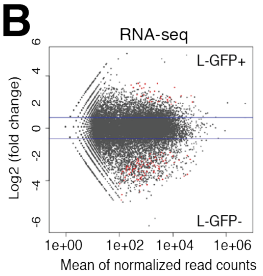

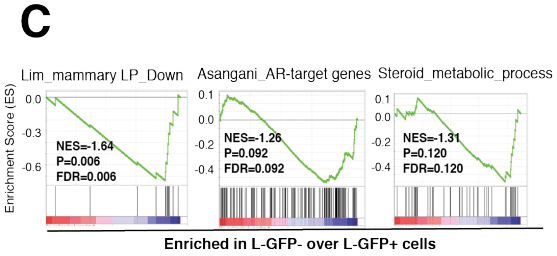

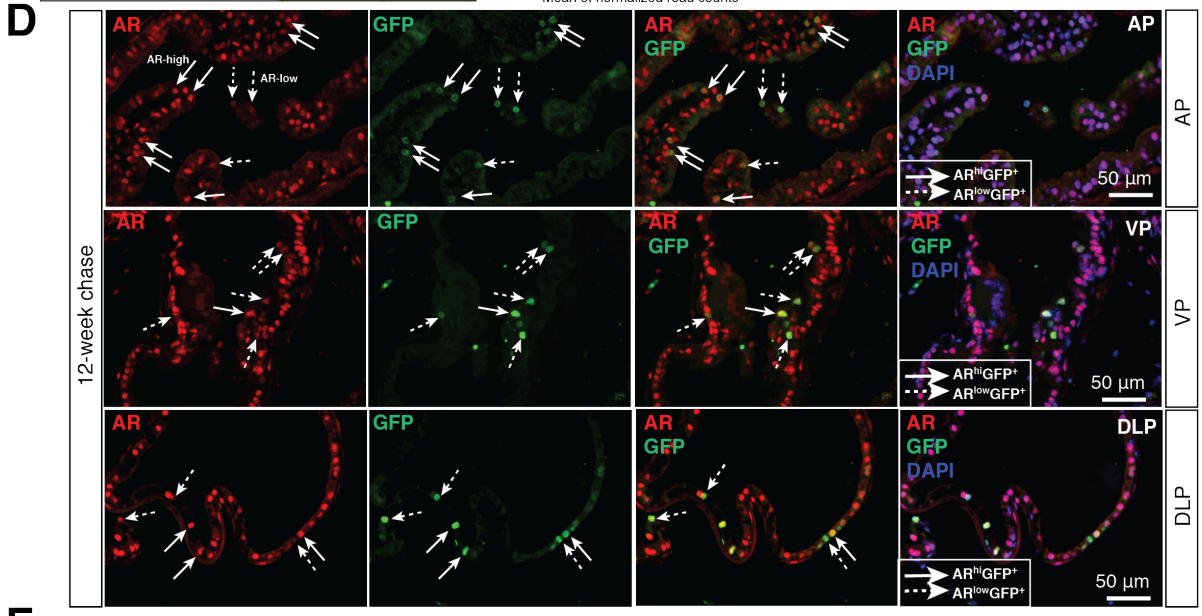

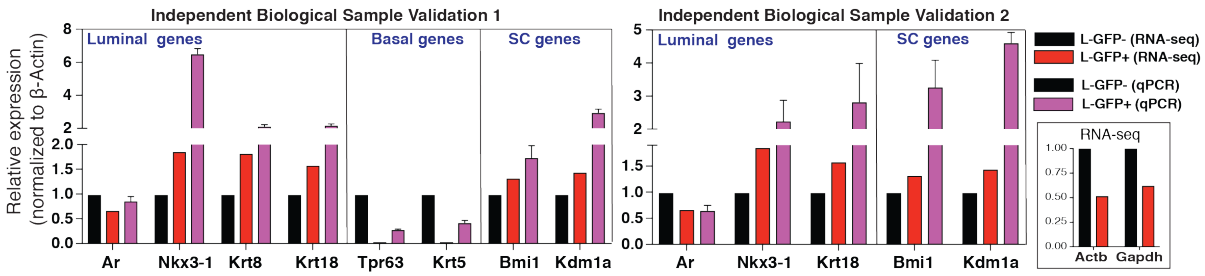

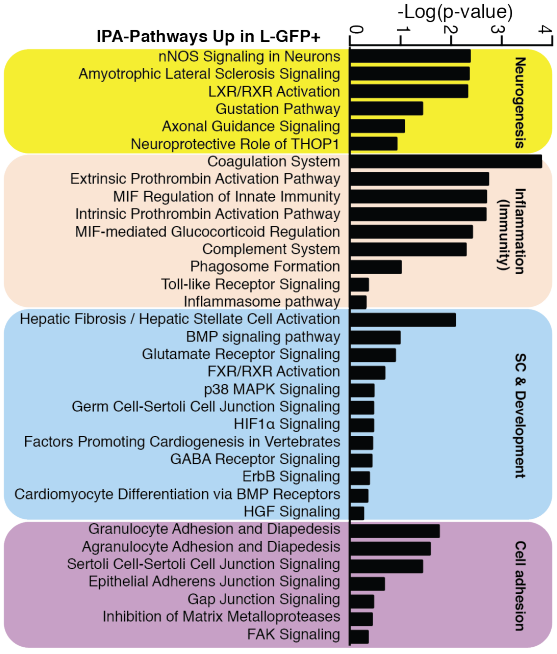

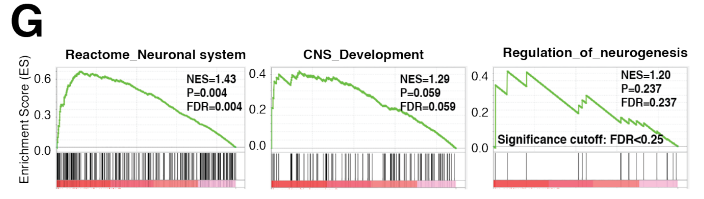

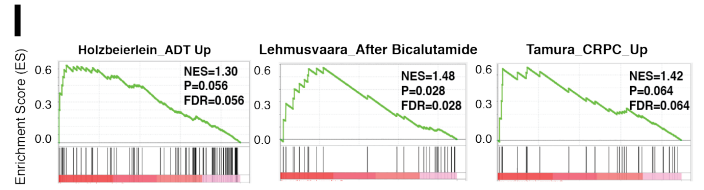

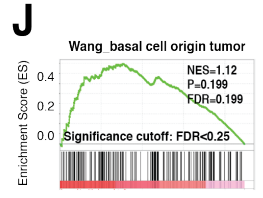

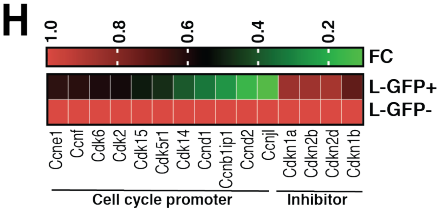

Figure S5. Luminal LRCs express unique progenitor cell gene signatures linked to CRPC, Related to Figure 5

(A) RNA-seq statistics.

(B) The MA plot showing appropriate normalization of our RNA-seq data.

(C) GSEA results showing the enrichment of indicated gene signatures in luminal GFP^- cells.

(D) Double IF staining of GFP and AR in prostates isolated from 12-week chased bigenic animals. Solid arrows point to GFP^+/AR^{hi} cells and dashed arrows to $GFP^{+/}AR^{low}$ cells.

(E) qRT-PCR validation of RNA-seq data. Two independently prepared sample pairs (luminal GFP^+ and GFP^- cells) were used in qRT-PCR analysis of several representative genes in 'luminal', 'basal', and 'SC' categories. Overall, the trend of gene expression was consistent between these two measurements with more dramatic differences detected by qPCR, which is reasonable as qPCR utilized Actb as normalization and tended to be more quantitative while RNA-seq did not use housekeeping gene expression for normalization. Note that both Actb and Gapdh mRNA expression levels were not evenly distributed in the L-GFP^+ and L-GFP^- cell populations in RNA-seq analysis (right boxed). Gene expression values in L-GFP^- cells detected by qPCR or RNA-seq were arbitrarily set as 1 for the purpose of comparison.

(F) Ingenuity pathway analysis (IPA) of genes preferentially upregulated in luminal GFP^+ cells.

(G) GSEA results showing the enrichment of indicated gene signatures in luminal GFP^+ cells.

(H) Heatmap of representative cell-cycle regulators in luminal GFP^+ and GFP^- cells. The relative gene expression values (i.e., fold change, FC) in L-GFP^+ over GFP- (arbitrarily set as 1) were used.

(I, J) GSEA results showing the enrichment of indicated gene signatures in luminal GFP^+ cells. Note that an FDR < 0.25 is statistically significant for GSEA analysis.

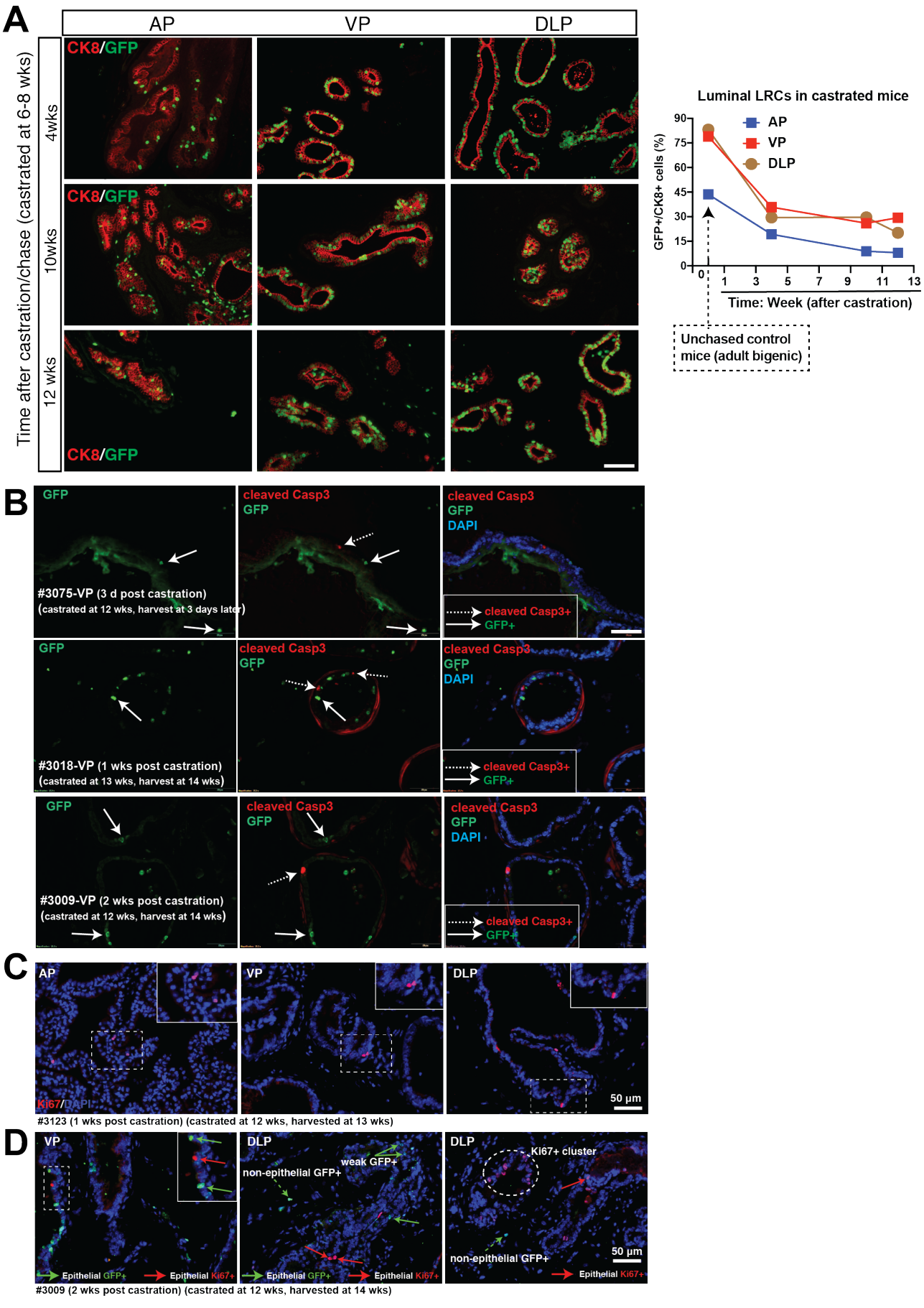
A
AP
VP
DLP
Time after castration/chase (castrated at 6-8 wks)
4wks
10wks
12 wks
CK8/GFP
Luminal LRCs in castrated mice
AP
VP
DLP
GFP+/CK8+ cells (%)
Time: Week (after castration)
Unchased control mice (adult bigenic)
B
GFP
cleaved Casp3
DAPI
#3075-VP (3 d post castration)
(castrated at 12 wks, harvest at 3 days later)
cleaved Casp3+
GFP+
#3018-VP (1 wks post castration)
(castrated at 13 wks, harvest at 14 wks)
#3009-VP (2 wks post castration)
(castrated at 12 wks, harvest at 14 wks)
C
AP
VP
DLP
Ki67/DAPI
50 μm
#3123 (1 wks post castration) (castrated at 12 wks, harvested at 13 wks)
D
non-epithelial GFP+
weak GFP+
Ki67+ cluster
Epithelial GFP+
Epithelial Ki67+
#3009 (2 wks post castration) (castrated at 12 wks, harvested at 14 wks)

Figure S6. Luminal LRCs mark androgen-independent cells and resist castration-induced apoptosis *in vivo*, Related to Figure 6

(A) Representative IF images and quantification of CK8 and GFP in different prostate lobes harvested from bigenic male mice castrated at 6-8 weeks and chased for 4, 10 and 12 weeks.

(B) IF of cleaved Caspase 3 and GFP in prostate tissues harvested from castrated mice. Different experimental settings, i.e., mice chased for 12 weeks were castrated and VP lobes harvested 3 days (top) or 2 weeks (bottom) later, or castrated at 13 weeks of chase and harvested 1 week later (middle panels) were employed to show that GFP^+ luminal LRCs were apoptosis-negative.

(C) IF of Ki67 in prostate tissues harvested from indicated castrated mice.

(D) IF of GFP and Ki67 in prostate tissues harvested from indicated castrated mice.

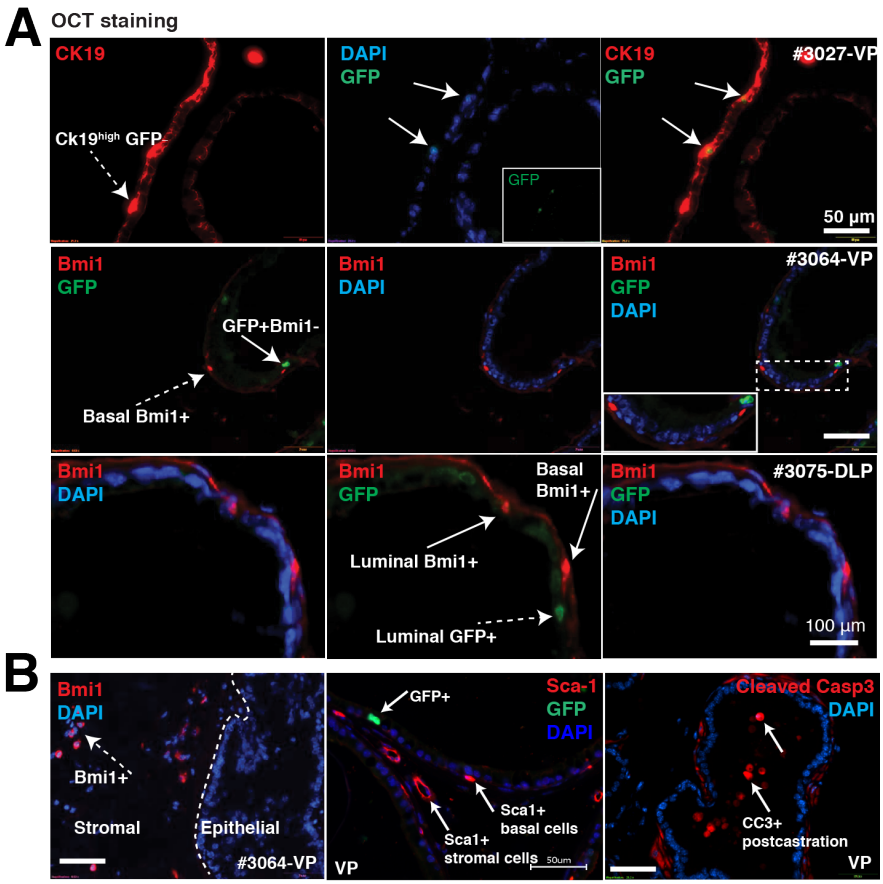

Figure S7. Phenotypic heterogeneity of luminal progenitor cells, Related to Figure 7

(A) Double IF staining of GFP and the indicated markers in frozen sections of prostate glands harvested from bigenic mice chased for 12 weeks. In the middle (right panel), the dashed boxed region is enlarged.

(B) Double IF of GFP and Bmi1 (left panel) or Sca-1 (middle panel) in FFPE sections obtained from bigenic mice chased for 12 weeks, and of GFP and cleaved Caspase 3 (CC3) in frozen tissue sections of prostate isolated from adult bigenic mice castrated for 1 week (right panel).

Table S1. Supporting data for quantitation of GFP^+ cell properties, Related to Figure 2, 4, 5, 6, S2, S6

Table S2. List of the differentially expressed genes (DEGs) in luminal GFP^- and GFP^+ cells (comparative to each other) isolated from 12-week chased bigenic mice in the RNA-Seq analysis, Related to Figure 5 and S5

Table S3. Antibodies and primers used in this study,
Related to Figure 1, 2, 4, 5, 6, 7, S1, S2, S3, S4, S5, S6, S7

Antibody	Supplier	Catalog. No	Species	Dilution
AR	EMD Millipore	06-680	Rabbit	1:750
Ck8	Developmental Studies Hybridoma Bank	TROMA-1	Rat	1:50
Ck5	Covance	PRB-1609	Rabbit	1:500
p63	Cell Signaling	4892S	Rabbit	1:500
Ki67	Leica Biosystems	NCL-Ki67p	Rabbit	1:500
Sox2	Cell Signaling	14962	Rabbit	1:150
GFP	Sigma	G6539	Mouse	1:500
GFP	Life Technologies	A-11122	Rabbit	1:1000
Ck19	Abcam	ab52625	Rabbit	1:200
Notch1	Abcam	ab52627	Rabbit	1:100
Stat3	Abcam	ab76315	Rabbit	1:150
Sca1	Abcam	ab109211	Rabbit	1:100
Cd117/c-Kit	Biolegend	105801	Rat	1:150
Cd14	Biolegend	150101	Rat	1:150
Cd133	Biolegend	141201	Rat	1:100
Notch3	R&D System	AF1308	Goat	1:100
Cd24	Santa cruz	sc-19585	Mouse	1:150
Bmi1	Millipore	05-637	Mouse	1:100
Hoxb9	Assay Biotech	C10404	Rabbit	1:150
Pbsn (M-18)	Santa Cruz	sc-17124	Goat	1:100
Casp3-cleaved	Cell Signaling	9664	Rabbit	1:150

Primer Name	Sequence (Forward 5'-3')	Sequence (Reverse 5'-3')
mGapdh	ATCACTGCCACCCAGAAGAC	AGGTTTCTCCAGGCGGCAC
mActb	AGCAAGCAGGAGTACGATGAG	AAGCCATGCCAATGTTGTC
mPbsn	TGCACAGTATGAAGGGAGCAT	GTCCGTGTCCATGATACGCT
mKrt5	GGGTCTTGGTTTGGGTAGCG	AGGCTCTTCTTAGCTCTTGAAG
mKrt14	GGAGATGATCGGCAGTGTGG	GAAGATGAAAGGTGGGCGT
mTrp63	GCTGCGTCGGAGGAATGAAC	TTGCTGCTTTCTGATGCTGTC
mKrt8	ACACTTTCAGCCGCACCAC	TCTCCCCGTGAGCCCTGA
mKrt18	GAGACGCACCCTCCAGACCT	GCTCCATCTGTGCCTTGTATC
mAr	GACCTGCTAATCAAGTCCCAT	ATTAGGGTTTCCAAATCTTCAC
mBmi1	TTATCAGCCATCAGTTATTTGTG	ACAGCAATGTGTGTAAAAGTAATG
mBcl2	CTACCGTCGTGACTTCGCAG	ACACACATGACCCCACCGA
mAldh1a1	TCAAGACAGTCGCAATGAAGAT	AAAACACGACTATGCTGGTTACTA
mAldh3a1	AGACATCAAGCGGTGGAGTG	AGACCTCACCAGGCAAGAGC
mLy6a	CAGCAGTTATTGTGGATTCTCA	CCTCCATTGGGAACTGCTAC
mNKX3-1	TCCCACCACTCAGTGCTATACAG	AACAAGGGACACGGAACAATAC
mVIM	AGCTGCTAACTACCAGGACACTA	CAGAGGAAGTGACTCCAGGTTAG
mSetdb1	TCAACCAACATGGCTTCCGT	CACCCAAGGGAAGCGAAGA
mKdm1a	GTATCTCGTTGGCGTGCTG	GCCCACTCAACAGAGCACCA
mCtnnb1	CCACCCTGGTGCTGACTATC	ATTTACAGGTCAGTATCAAACCAG

Note: "m" means mouse.

Supplemental Experimental Procedures

Generation of Prostate-Specific Pb-tetVP16-GFP Transgenic Mice

General procedures in producing and propagating transgenic animals have been previously described (Suraneni et al., 2010). Briefly, we adopted a modified tetracycline-repressible histone H2B-GFP (Tet-off) system previously used to assess slow-cycling stem cells in the skin (Tumbar et al., 2004) to monitor GFP dynamics as readout of cell cycle frequency in prostate epithelial cells. Transgene constructs (Figure S1A) were prepared by placing tetR-VP16 (pTET-Off, BD Biosciences Clontech) under the control of prostate specific and androgen responsive composite *probasin* promoter ARR2PB (Zhang et al., 2000) with an intervening rabbit b-globin second intron sequence to augment transgene expression and followed by b-globin–SV40 hybrid polyA sequences for transcript stability (Chen et al., 2009). This ARR2PB-tetR-VP16 line were bred with tetO-HIST1H2BJ/GFP (H2B-GFP) mice (stock # 005104, Jackson Laboratory), in which expression of H2B-GFP is under the control of the TET response element (TRE), to generate Pb-tetVP16-GFP bigenic mice (Figure S1A). To analyze the decay of H2B-GFP signal, young adult bigenic male mice were fed DOX chow (2 g/kg body weight, Teklad) starting at 6 weeks and were kept on DOX food for entire chase period (6-18 weeks).

Colony and Sphere Formation Assays

For colony formation assays (Zhang et al., 2011; Zhang et al., 2016), we plated freshly purified prostate epithelial cells at a low density (i.e., 1,000-10,000 cells/well) in 6-well plate precoated with PureCol (Advanced BioMatrix, San Diego, CA), and let cells grow for 7-10 days before the visualization of the culture by crystal violet staining. For sphere-formation assays (Liu et al., 2011), cells were suspended in 1:1 Matrigel (BD Biosciences, San Jose, CA)/medium in a total volume of 100 µl. The mixtures were then plated around the rims of wells in a 12-well plate and allowed to solidify in 37°C incubator for 25 minutes, followed by addition of 1 ml of warm medium. Usually 7-9 days after plating, spheres with a diameter over 50 µm were counted. PrEGM and modified WIT medium capable of propagating prostatic stem-like cells (inducing luminal progenitors) was used for 2D culture (Zhang et al., 2017) whereas both WIT and recently established prostate organoid medium (Karthaus et al., 2014) were used for 3D sphere/organoid cultures. For all experiments, we ran a minimum of triplicate wells for each condition and repeated experiments 2-4 times.

Histology, Immunofluorescence (IF) Staining, and Microscopy

Hematoxylin and eosin (H&E) and IF staining was performed on either 5-µm paraffin-embedded or OCT frozen sections. Basic IF procedures have been described previously (Jeter et al., 2009). The coverslips or the tissue slides were blocked with Background Sniper (Biocare Medical, Concord, CA) for 30 minutes, followed by primary antibody incubation overnight at 4°C. Primary antibodies and dilutions used are listed in Table S3. Slides were then incubated with secondary antibodies (diluted 1:700 in antibody diluent (Dako, Carpinteria, CA)) labeled with AlexaFluor 488 or 594 (Invitrogen/Molecular Probes, Grand Island, NY). After washing (3X) with PBS, sections were counterstained with 4,6-diamidino-2-phenylindole (DAPI) (Sigma-Aldrich, St. Louis, MO) and mounted with ProLong® Gold Antifade Mountant (Life Technologies, Grand Island, NY). For quantification of AR staining intensity in luminal GFP^+ cells, a serial dilution of AR antibody from 1:100 to 1:750 was tested and 1:750 dilutions was selected. H&E and IF images were captured by Olympus IX71, and Keyence BZ-X700 and Zeiss LSM510 META confocal microscope, respectively.

Mouse Prostate Tissue Disassociation and Flow Cytometry

Prostate tissues were dissected and minced to small clumps, followed by enzymatic dissociation with collagenase IA (200 U/ml) and Dispase (1 U/ml) in DMEM media with 10% FBS and 10 µM of p160ROCK inhibitor Y-27632 dihydrochloride (Selleckchem, Houston, TX) for 90 min. Dissociated tissue was then treated with 0.2% Trypsin for 10 min followed by 35 min DNase I (0.1 mg/mL) digestion in 37℃. After passing sequentially through 21- and 23- gauge needles, cells were filtered by a 40-µm cell strainer to obtain single-cell suspensions. A mouse lineage cell depletion (order # 130-090-858, Myltenyi Biotech) step was applied according to manufacturer's instruction. The resultant cells were stained for 30 min at 4℃ with PE-CD49f and APC-Sca-1 (eBioscience, San Diego, CA). FACS was performed by using the BD Aria or Fusion (BD Biosciences, San Jose, CA). PI (Propidium iodide) or 7-AAD was added prior to FACS analysis to separate viable from dead cells. As described previously (Valdez et al., 2012), three major populations were defined on the FACS profile as basal ($Sca\text{-}1^+CD49f^{hi}$), luminal ($Sca\text{-}1^-CD49f^{lo}$) and stromal ($Sca\text{-}1^+CD49f^{-/lo}$) cells. For the majority of the experiments, GFP^+ and GFP^- cells were specifically sorted out from the luminal population.

Prostate Tissue Regeneration Assays

Tissue regeneration assays were performed as described (Xin et al., 2003). Briefly, varying number of freshly disassociated prostatic cells or FACS-purified cells were combined with $1.0\sim2.0 \times 10^5$ mouse or rat urogenital sinus mesenchyme (UGM)

in collagen and injected subcutaneously or under the kidney capsule. The outgrowths were harvested for analysis from the experimental mice 2~3 months later.

RNA Isolation and Quantitative RT-PCR (qPCR)

Total RNA was isolated from cells using the RNeasy mini kit (Qiagen, Valencia, CA). The first-strand cDNA synthesis was achieved by reverse transcription of RNA using random hexamers and SuperScript III Reverse Transcriptase (Invitrogen, Grand Island, NY). Quantitative RT-PCR was performed using the iQ™ SYBR® Green supermix (BioRad, Hercules, CA) on a 7900HT Fast Real-Time PCR System (ABI, Applied Biosystems, Foster City, CA). The primers used in this study are listed in Table S3. The housekeeping gene Gapdh or Actb was used as internal control for gene expression normalization.

RNA Sequencing (RNA-seq) and Bioinformatics

For RNA-Seq analysis, freshly purified GFP^+/GFP^- luminal cells were subjected to total RNA extraction using an RNeasy mini kit (Qiagen, Valencia, CA). cDNA libraries were constructed using the TruSeq Stranded Total RNA Preparation Kit (Illumina, cat#: RS-122-2301), which contained Ribo-Zero™ Gold to deplete rRNA. We only amplified our libraries for 10 PCR cycles (instead of 15 suggested by manufacturer) to minimize amplification-induced noise. Purified libraries were quantified using a Kapa library quantification kit (KAPA Biosystems, Wilmington, MA) and then loaded onto a cBot (Illumina, San Diego, CA) at a final concentration of 10 pM to perform cluster generation, followed by 2 x 75 bp sequencing on a HiSeq 2000 (Illumina, San Diego, CA). Two libraries were loaded per lane, yielding an average of 77 M pairs of reads per sample. We mapped the sequencing reads to the reference mouse genome (mm10) using TopHat (version 2.0.10) (Kim et al., 2013) and Bowtie 2 (version 2.1.0) (Langmead and Salzberg, 2012). The number of fragments in each known gene from GENCODE Release M7 (Mudge and Harrow, 2015) was enumerated using htseq-count from HTSeq package (version 0.6.0) (Anders et al., 2015). Genes with fewer than 10 fragments in all samples were removed before differential expression analysis. Differential expression between conditions was statistically assessed by R/Bioconductor package DESeq (version 1.16.0) (Anders and Huber, 2010). Due to the rarity of sorted cells, one sample pooled from multiple sorting was collected for RNA-seq analysis for each cell type. To call differentially expressed genes (DEGs), we used fold change (FC) $\geq$6 and normalized read counts $\geq$20 for bulk luminal GFP^- cells, and FC $\geq$4 and normalized read counts $\geq$10 for rare luminal GFP^+ LRCs. These criteria generated a manageable list of 929 genes preferentially expressed in GFP^+ cells and 1303 genes in GFP^- cells (Table S2).

For Gene Ontology analysis, IPA (Qiagen, Valencia, CA) and DAVID version 6.7 (Huang da et al., 2009) were used with gene symbols. GSEA (the pre-rank function) was carried out by using the curated gene sets (C2) of the Molecular Signature Database (MSigDB) version 4.0 provided by the Broad Institute (http://www.broad.mit.edu/gsea/) (Subramanian et al., 2005). Note that the list of DEGs and entire detectable genes derived from each sample were used for IPA/GO and GSEA analysis, respectively. In particular, we followed the standard procedure as described by GSEA user guide (http://www.broadinstitute.org/gsea/doc/GSEAUserGuideFrame.html). The FDR for GSEA is the estimated probability that a gene set with a given NES (normalized enrichment score) represents a false positive finding, and an FDR <0.25 is statistically significant for GSEA analysis. To reconcile the difference between mouse and human species, the "gene_symbol.chip" function was employed to collapse dataset to gene symbols when performing GSEA. The RNA-Seq data reported in this paper is available in the Gene Expression Omnibus (GEO) database under accession number GSE98760.

Supplemental References

Anders, S., and Huber, W. (2010). Differential expression analysis for sequence count data. Genome biology *11*, R106.
Anders, S., Pyl, P.T., and Huber, W. (2015). HTSeq: a Python framework to work with high-throughput sequencing data. Bioinformatics *31*, 166-169.

Chen, X., Schneider-Broussard, R., Hollowell, D., McArthur, M., Jeter, C.R., Benavides, F., DiGiovanni, J., and Tang, D.G. (2009). Abnormal differentiation, hyperplasia and embryonic/perinatal lethality in BK5-T/t transgenic mice. Differentiation *77*, 324-334.

Huang da, W., Sherman, B.T., and Lempicki, R.A. (2009). Systematic and integrative analysis of large gene lists using DAVID bioinformatics resources. Nat. Protoc. *4*, 44-57.

Jeter, C.R., Badeaux, M., Choy, G., Chandra, D., Patrawala, L., Liu, C., Calhoun-Davis, T., Zaehres, H., Daley, G.Q., and Tang, D.G. (2009). Functional evidence that the self-renewal gene NANOG regulates human tumor development. Stem Cells *27*, 993-1005.

Karthaus, W.R., Iaquinta, P.J., Drost, J., Gracanin, A., van Boxtel, R., Wongvipat, J., Dowling, C.M., Gao, D., Begthel, H., Sachs, N.*, et al.* (2014). Identification of multipotent luminal progenitor cells in human prostate organoid cultures. Cell *159*, 163-175.

Kim, D., Pertea, G., Trapnell, C., Pimentel, H., Kelley, R., and Salzberg, S.L. (2013). TopHat2: accurate alignment of transcriptomes in the presence of insertions, deletions and gene fusions. Genome Biol. *14*, R36.

Langmead, B., and Salzberg, S.L. (2012). Fast gapped-read alignment with Bowtie 2. Nature methods *9*, 357-359.
Liu, C., Kelnar, K., Liu, B., Chen, X., Calhoun-Davis, T., Li, H., Patrawala, L., Yan, H., Jeter, C., Honorio, S.*, et al.* (2011). The microRNA miR-34a inhibits prostate cancer stem cells and metastasis by directly repressing CD44. Nat. Med. *17*, 211-215.

Mudge, J.M., and Harrow, J. (2015). Creating reference gene annotation for the mouse C57BL6/J genome assembly. Mamm. Genome *26*, 366-378.

Subramanian, A., Tamayo, P., Mootha, V.K., Mukherjee, S., Ebert, B.L., Gillette, M.A., Paulovich, A., Pomeroy, S.L., Golub, T.R., Lander, E.S.*, et al.* (2005). Gene set enrichment analysis: a knowledge-based approach for interpreting genome-wide expression profiles. Proc. Natl. Acad. Sci. USA *102*, 15545-15550.

Tumbar, T., Guasch, G., Greco, V., Blanpain, C., Lowry, W.E., Rendl, M., and Fuchs, E. (2004). Defining the epithelial stem cell niche in skin. Science *303*, 359-363.

Valdez, J.M., Zhang, L., Su, Q., Dakhova, O., Zhang, Y., Shahi, P., Spencer, D.M., Creighton, C.J., Ittmann, M.M., and Xin, L. (2012). Notch and TGFbeta form a reciprocal positive regulatory loop that suppresses murine prostate basal stem/progenitor cell activity. Cell Stem Cell *11*, 676-688.

Xin, L., Ide, H., Kim, Y., Dubey, P., and Witte, O.N. (2003). In vivo regeneration of murine prostate from dissociated cell populations of postnatal epithelia and urogenital sinus mesenchyme. Proc. Natl. Acad. Sci. USA *100 Suppl 1*, 11896-11903.

Zhang, D., Jiang, P., Xu, Q., and Zhang, X. (2011). Arginine and glutamate-rich 1 (ARGLU1) interacts with mediator subunit 1 (MED1) and is required for estrogen receptor-mediated gene transcription and breast cancer cell growth. J. Biol. Chem. *286*, 17746-17754.